European Journal of Radiology Open 8 (2021) 100383

Contents lists available at ScienceDirect

European Journal of Radiology Open

journal homepage: www.elsevier.com/locate/ejro

Anatomical analysis of inflammation in hand psoriatic arthritis by Dual-Energy CT Iodine Map

Sho Ogiwara *, Takeshi Fukuda, Reina Kawakami, Hiroya Ojiri, Kunihiko Fukuda

Department of Radiology, The Jikei University School of Medicine, Tokyo, Japan

HIGHLIGHTS

- Dual-Energy CT (DECT) Iodine Map has high iodine contrast resolution with maintaining high spatial resolution.
- Variable enthesitis of peripheral joints may be key findings for diagnosis of psoritatic arthritis (PsA).
- DECT Iodine Map allowed to determine precise anatomical structures of inflammation in hand PsA.

ARTICLE INFO

Keywords:
Psoriatic arthritis
Dual-Energy CT
MRI
Synovitis
Enthesitis

ABSTRACT

Objective: This study aimed to identify the detailed location of inflammatory lesions and its frequency of hand PsA on DECT Iodine Map with referring the cadaveric specimen.
Materials and methods: Thirty-eight anatomical landmarks were selected as a potential inflammatory sites in the thumb and middle finger. We included 22 symptomatic PsA patients who underwent contrast enhanced DECT of the hand. MR images and macroscopic specimens of thumb and middle finger were prepared from a cadaver. Two musculoskeletal radiologists evaluated DECT with referring the cadaveric images to determine the precise location of inflammatory sites and its frequency.
Results: The frequently observed inflammation sites of active PsA patients were either classical or functional entheses, and coincide with the well-known hypothesis that primary inflammatory sites of PsA are enthesis. We have noticed that there was remarkable enhancement around DIP joints (13.6 %–45.5 %).
Conclusion: DECT could assess the detailed anatomical sites of the inflammatory lesion in hand psoriatic arthritis, which coincided with enthesis.

1. Introduction

Psoriatic arthritis (PsA), along with rheumatoid arthritis (RA), is a common inflammatory arthritis of the small joints of the hands and feet [1]. Since early diagnosis allows early intervention of biologics and good therapeutic efficacy, there is a need for imaging studies that can evaluate early signs of enthesitis and synovitis with an ability to analyze treatment response [2,3].

We reported that Dual-Energy CT (DECT) Iodine Map enables delineation of inflammatory changes with good iodine contrast and high spatial resolution in short examination times [4]. The main locus of inflammation is thought to be different in RA and PsA. In PsA, entheses, which has been regarded as the main locus of inflammation, are present all over the finger. The location of inflammation is important in the pathogenesis of PsA and differentiating from RA. This difference is thought to create different image findings, as shown in the Table1. In this regard, DECT may evaluate precise inflammatory sites with high spacial resolution that CT has.

If the detailed anatomical inflammatory sites could be analyzed, a deeper understanding of the pathogenesis of PsA may be possible. However, detailed anatomical analysis of inflammatory sites with DECT Iodine Map has not been conducted.

Moreover, our previous study showed that the enhancement around distal interphalangeal joint (DIP) was more frequently observed on DECT Iodine Map compared to contrast-enhanced MR (CE-MR) imaging in PsA patients [5]. It is still undetermined whether this phenomenon was a false positive or true inflammatory lesion.

The purpose of this study was to identify the detailed location of

* Corresponding author at: ParkAxis Nakaokachimachi #1002, 3-5-3, Taitou, Taitouku, Tokyo, 110-0016, Japan.
E-mail address: a-h-s-ogiwara@mrj.biglobe.ne.jp (S. Ogiwara).

https://doi.org/10.1016/j.ejro.2021.100383
Received 11 August 2021; Received in revised form 29 September 2021; Accepted 7 October 2021

Table 1
Typical findings of RA and PsA in MRI, US and DECT.

	RA	PsA
MR imaging	Joint capsule synovitis Tenosynovitis Bone marrow edema Bone erosion Joint space narrowing	Enthesitis Joint capsule synovitis Tenosynovitis and peritendinitis Periarticular inflammation Bone marrow edema Bone erosion/bone proliferation
US	Same as MRI but unable to detect bone marrow edema	Same as MRI but unable to detect bone marrow edema
DECT	Same as MRI but unable to detect bone marrow edema of small bones	Same as MRI but unable to detect bone marrow edema of small bones

inflammatory lesion and its frequency of hand PsA on DECT Iodine Map through comparison with gross anatomy, high resolution MR imaging, and Iodine Map of cadaveric fingers.

2. Materials and methods

2.1. Subjects

2.1.1. Patients

We included consecutive symptomatic PsA patients who presented at the dermatology outpatient clinic of our institution from June 2014 to July 2017. Subjects who underwent DECT at our institution before therapeutic intervention were included. PsA cases without the involvement of hands were excluded. Finally, we included 22 cases for this study.

2.1.2. Cadaver

Formalin-alcohol fixed cadaveric hand of an 80-year-old male without a history of joint disease was prepared. The thumb and middle finger were scanned with MR imaging, and cadaveric gross specimens of the middle finger were prepared.

2.2. DECT protocol for PsA patients

All patients underwent scanning with the SOMATOM Definition Flash (Siemens Healthineers, Forchheim, Germany) in dual energy mode with following parameters: tube energy of 80 kV and 140 kV with 0.4 mm tin filter, 250 and 125 effective mAs, 0.5-second rotation time, 40 × 0.6-mm collimation, and pitch of 0.6.

The contrast medium, Iohexol 100 mL (Omnipaque, 350 mg of iodine per milliliter; Daiichi-Sankyo, Tokyo, Japan) was injected from the antecubital vein at a rate of 1.5 mL/sec. Scan was started 120 s after injection.

All images were reconstructed from DE data with 1.0-mm-thick sections in 0.7-mm increments. A commercial workstation (Syngo Dual Energy, Liver VNC; Siemens Healthineers) was used for three-material decomposition analysis and to make the Iodine Map. The image was reconstructed in three orthogonal planes for each finger. Window center and window width of images were fixed as 55 and 70 Hounsefield unit (HU), respectively, for image standardization.

2.3. Imaging for cadaveric finger

Cadaveric fingers were scanned with MR imaging and DECT.

MR Images were obtained by using 1.5-T unit, either the MAGNETOM Avanto (Siemens Healthineers, Erlangen, Germany) or the MAGNETOM Symphony with Tim System (Siemens Healthineers). Proton density weighted image (PDWI) in three orthogonal planes where obtained (Repeating Time;4500 msec, Echo Time;24 msec). Slice thickness were set at 1 mm.

Cadaveric gross specimens of the middle finger were prepared in axial section of the metacarpophalangeal (MCP) joint and mid-sagittal section from the proximal interphalangeal (PIP) to the tip of the finger.

After diluted Iohexol (Omnipaque, 350 mg of iodine per milliliter; Daiichi-Sankyo, Tokyo, Japan) with saline at 1/200 was applied on the inner lining of the articular capsule of the MCP-DIP joint where the capsular synovitis can be occurred, DECT Iodine Map was obtained by using the same protocol as for the PsA patinets.

Table 2
The anatomical structure evaluated.

Middle finger		Thumb	
Metacarpo-phalangeal joint	Lumbrical muscle/ interosseous muscle	Metacarpo-phalangeal joint	Abductor pollicis brevis
	Sagital band		Flexor pollicis brevis
	A1 pulley		Adductor pollicis muscle
	Articular capsule		Extensor pollicis brevis
	Medial collateral ligament		Sagital band
	Lateral collateral ligament		Medial collateral ligament
	Volar plate		Lateral collateral ligament
Proximal phalanx	A2 pulley		Volar plate
	Transverse retinacular band		Articular capsule
	C1 pulley		Extensor pollicis longus
Proximal interphalangeal joint	Articular capsule	Interphalangeal joint	Flexor pollicis longus
	Medial collateral ligament		Medial collateral ligament
	Lateral collateral ligament		Lateral collateral ligament
	Volar plate		Articular capsule
Middle phalanx	Insertion of central slip		Volar plate
	Insertion of flexor digitorum superficialis		
	A4 pulley		
	Insertion of conjoined tendon		
	Incertion of flexor digitorum profundus		
Distal interphalangeal joint	Articular capsule		
	Medial collateral ligament		
	Lateral collateral ligament		
	Volar plate		

Table 3
Patient Characteristics.

	n
Mean age	54.8 (±17.6)
Gender (M:F)	15:7
Fulfilled CASPER criteria	22 (100 %)
Mean psoriasis duration (year)	11.8 (±11.3)
Mean joint symptom duration (month)	19.5 (±35.6)
Nail change	14 (64 %)

2.4. Image analysis

DECT Iodine Map of the thumbs and middle fingers of 22 PsA patients were evaluated for the presence of iodine accumulation in 38 periarticular anatomical structures by 2 musculoskeletal (MSK) radiologists (S.O. and K.F., with 8 and 27 years of experience in interpreting musculoskeletal CT and MR images, respectively). The evaluated 38 anatomical structures are shown on the Table 2. To determine which anatomy corresponds to the sites of iodine accumulation on DECT Iodine Map, gross specimens and high-resolution MR images of cadaveric fingers, and also DECT Iodine Map of iodine applied cadaveric fingers were used as references. Through the discussion by the 2 MSK radiologists, the frequency of iodine accumulation in each anatomical structure was calculated.

3. Results

3.1. Patient characteristics

A total of 22 patients who had symptomatic PsA of digital joints and completed DECT were included. The group included 15 men and 7 women, with a mean age of 54.8 (±17.6) years. The mean duration of psoriasis was 11.8 (± 11.3) years, and the mean joint symptom duration was 19.5 (±35.6) months. All subjects fulfilled Classification Criteria for Psoriatic Arthritis (CASPAR) criteria. The demographic and clinical characteristics of enrolled patients are shown in Table 3.

Table 4
The detection rate of iodine accumulation assessed by MSK radiologist.

Middle finger		Detection frequency	Thumb		Detection frequency
Metacarpo-phalangeal joint	Lumbrical muscle/interosseous muscle	13.6 %	Metacarpo-phalangeal joint	Abductor pollicis brevis	4.5 %
	Sagital band	13.6 %		Flexor pollicis brevis	4.5 %
	A1 pulley	18.2 %		Adductor pollicis muscle	9.1 %
	Articular capsule	9.1 %		Extensor pollicis brevis	9.1 %
	Medial collateral ligament	13.6 %		Sagital band	22.7 %
	Lateral collateral ligament	9.1 %		Medial collateral ligament	9.1 %
	Volar plate	9.1 %		Lateral collateral ligament	4.5 %
Proximal phalanx	A2 pulley	22.7 %		Volar plate	9.1 %
	Transverse retinacular band	13.6 %		Articular capsule	0%
	C1 pulley	22.7 %		Extensor pollicis longus	22.7 %
	Articular capsule	4.5 %		Flexor pollicis longus	13.6 %
Proximal interphalangeal joint	Medial collateral ligament	22.7 %	Interphalangeal joint	Medial collateral ligament	18.2 %
	Lateral collateral ligament	18.2 %		Lateral collateral ligament	13.6 %
	Volar plate	13.6 %		Articular capsule	0%
	Insertion of central slip	9.1 %		Volar plate	4.5 %
Middle phalanx	Insertion of flexor digitorum superficialis	18.2 %			
	A4 pulley	27.2 %			
	Insertion of conjoined tendon	22.7 %			
	Incertion of flexor digitorum profundus	13.6 %			
Distal interphalangeal joint	Articular capsule	36.4 %			
	Medial collateral ligament	45.5 %			
	Lateral collateral ligament	36.4 %			
	Volar plate	13.6 %			

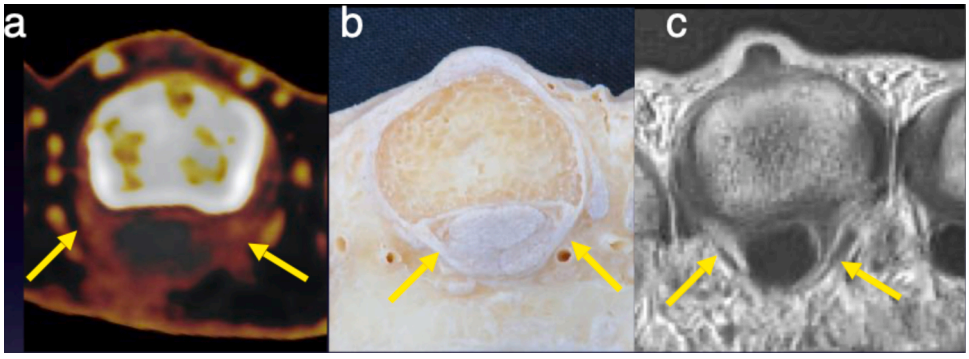

Fig. 1. A 28-year-old man with PsA.
a) Axial DECT Iodine Map shows iodine accumulation consistent with the A1 pulley on the palmar side of MCP joint (arrow).
b) Axial section of the gross cadaveric specimen and c) axial section of PDWI image of the cadaver delineates the corresponding A1 pulley (arrow).

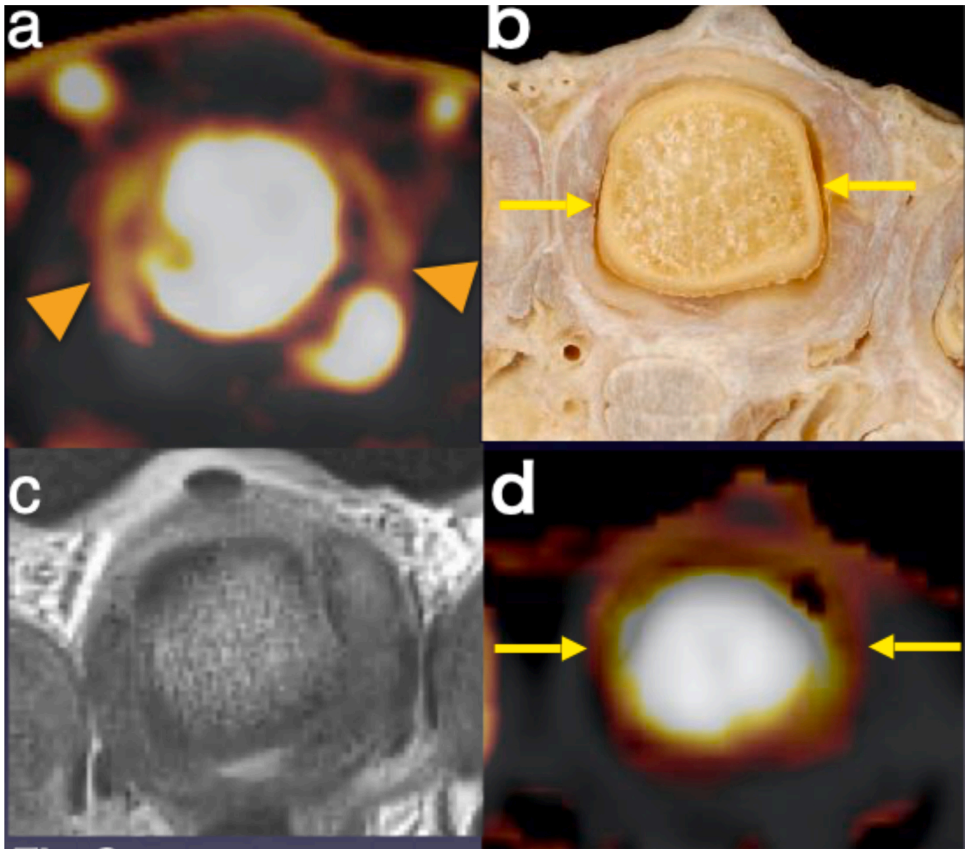

Fig. 2. a) Axial DECT Iodine Map of the middle finger MCP joint from 28-year-old man with PsA demonstrates linear enhancement along the articular capsule, suggestive of capsular synovitis (arrowhead).
b) Axial section of cadaveric specimen shows capsular synovium as a circular structure (arrow) surrounding metacarpal head.
c) Corresponding axial PDWI delineates synovium that is in close relationship with metacarpal head.
d) DECT Iodine Map was obtained after application of diluted contrast medium on the inner articular capsule surface (arrow). Linear enhancement similar to the capsular synovitis of the case was delineated.

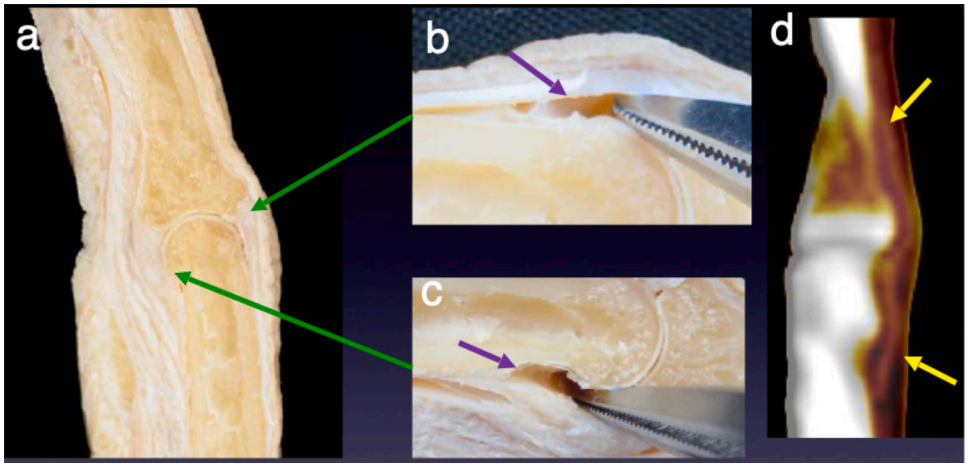

Fig. 3. a) Sagittal section of the PIP joint from cadaveric finger.
b) Dorsal and c) volar joint space was determined. We applied diluted iodine contrast to the inner surface of the joint capsule.
d) Coronal section of DECT Iodine Map of the cadaver after application of contrast medium application shows linear enhancement (arrow), similar to that of previous case.

3.2. Assessment of iodine accumulation of each anatomical structure

The frequency of iodine accumulation in each anatomical structure is shown in Table 4.

3.2.1. Pulley system

Many pulleys are known to exist on the palmar side of the fingers, that support the function of the flexor tendon. DECT Iodine Map showed abnormal enhancement along the pulleys, which could be regarded as functional enthesitis (Fig. 1). The frequency of inflammation was relatively high at all pulleys we assessed (18.2 %–27.2 %) and inflammation tended to be more prevalent in the distal part.

3.2.2. Joint capsules

Synovitis in PsA tended to show linear enhancement along the joint capsule synovium. They were similar to DECT Iodine Map of cadaveric finger joint after application of diluted contrast medium on the inner articular capsule surface (Figs. 2 and 3). Our results showed varying detection frequency of joint capsules. In the thumbs, the frequency was 0 %. On the other hand, the linear enhancement along the joint capsule was detected in the middle fingers and the highest frequency showed in the DIP joint (MCP 9.1 %, PIP 4.5 %, DIP 36.4 %).

3.2.3. Collateral ligament

The inflamed collateral ligament enthesis was also delineated on DECT Iodine Map with its high spatial resolution and thin slice

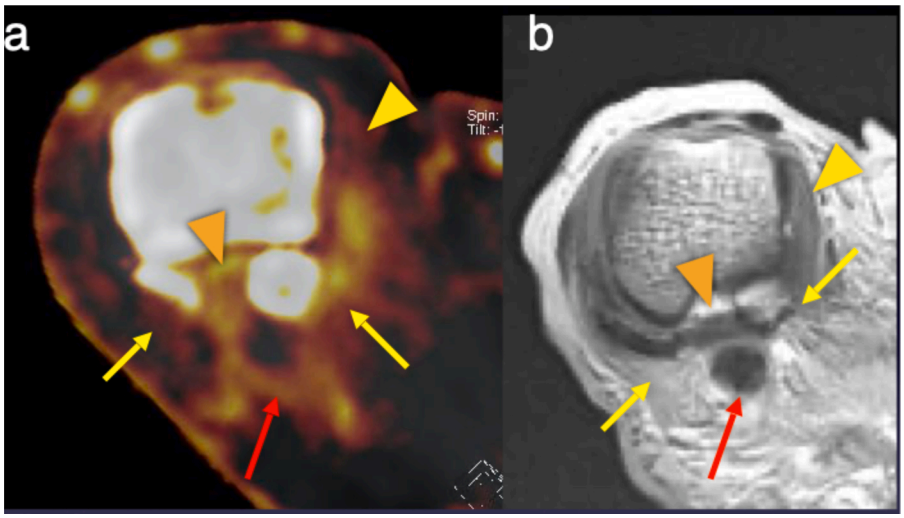

Fig. 4. A 80-year-old female with PsA.
a) Axial section of DECT Iodine Map shows contrast enhancement to the palmar structures of the MCP joint such as the enthesis of flexor pollicis brevis, adductor pollicis muscle and abductor pollicis brevis (yellow arrow), the volar plate. (arrowhead), the flexor tendon (red arrow), and the medial collateral ligament (yellow arrow head).
b) Axial section of PDWI from cadaveric finger delineate corresponding structures.

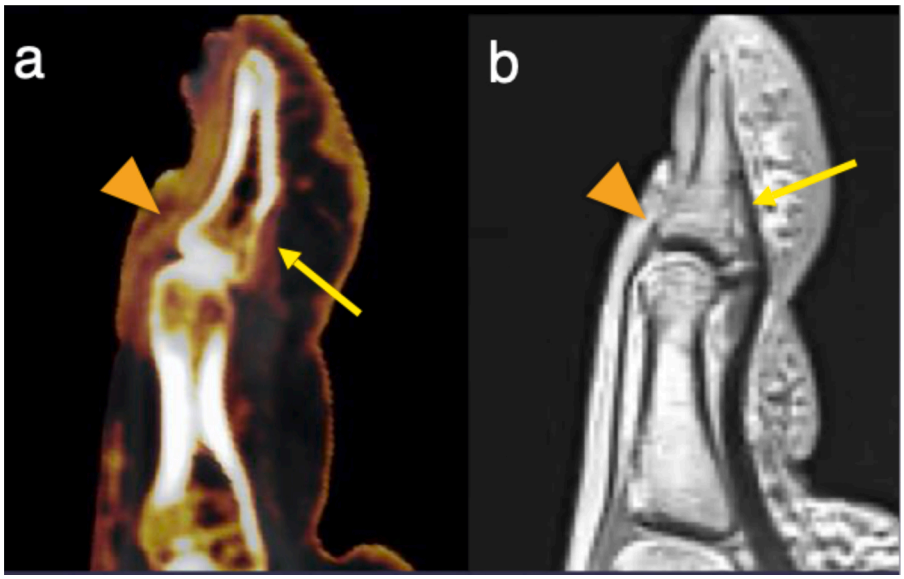

Fig. 5. A 80-year-old female with PsA.
a) Sagittal DECT Iodine Map of the first IP joint shows inflammation at the attachment site of the flexor tendon (arrow) and the extensor tendon (arrowhead). Severe nail deformity and abnormal nail bed enhancement are also noticed.
b) Attachment site of the flexor and extensor tendon is identified on corresponding PDWI of the cadaveric finger.

thickness. The collateral ligament consists of the radial and ulnar side wall of the joint capsule.

3.2.4. Enthesis of the flexor and extensor tendon

In the thumb, the extensor pollicis brevis tendon inserts onto the dorsal base of the proximal phalanx and the extensor pollicis longus tendon continues distally and inserts onto the dorsal base of the distal phalanx. The flexor pollicis brevis tendon inserts onto the radial sesamoid bone and radial base of the proximal phalanx with abductor pollicis brevis. The flexor polices longus tendon inserts onto the base of the distal phalanx. Cadaveric high resolution MR image showed these enthesis. Despite the considerable anatomical complexity, DECT managed to distinguish each inflamed anatomical structure. (Fig. 4).

In the other digit, extensor tendons which originate from both extrinsic and intrinsic extensor muscles create central slip and terminal tendon through complex connectivity. Inflammation of extensor tendon enthesis at the base of distal phalange was relatively frequent (22.7 %) and could spread to nail bed continuously (Fig. 5).

The flexor tendon consists of two tendons: the flexor digitorum superficialis, which inserts on the midportion of the middle phalanx, and the flexor digitorum profundus, which inserts on the volar base of the distal phalanx. Not only attachment sites of the tendon, but also enhancement along tendon sheath was detected as tenosynovitis (Fig. 6).

4. Discussion

The current study revealed that the frequently observed inflammation sites of active PsA patients could be classified as either classical or functional entheses. In the thumb, sagittal band around the MCP joints, medial collateral ligament of the IP joints, and around the extensor pollicis longus tendon were the three most prevalent sites. In the middle finger, variable pulleys, collateral ligaments, and articular capsule of the PIP joints, and various entheseal stuructures in the DIP joints were dominant inflammatory sites. Functional enthesis, coined by Benjamin and McGonagle, is referred to the sites where tendons and ligaments wrap around bony pulleys - i.e. regions where the bones and tendons/ligaments are closely in contact but not attached [6]. Pulleys and sagittal band are representative tissue of functional enthesis of the fingers whereas the attachment sites of tendon and ligament are named as classical enthesis. Enhancement along tendon sheath was seen occasionally on DECT Iodine Map. Because tendon sheath has synovium,

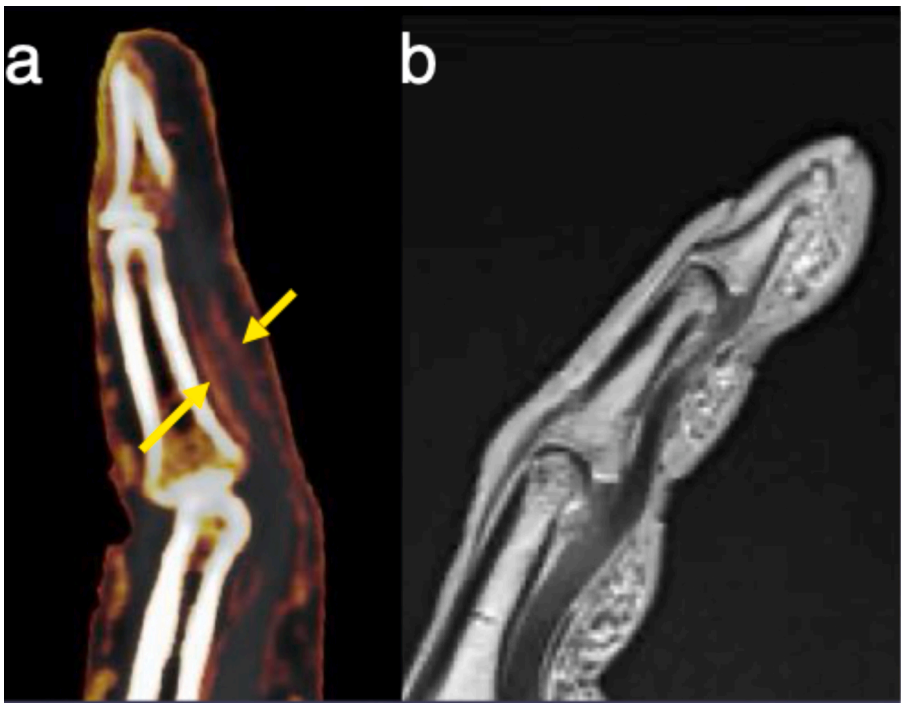

Fig. 6. A 68-year-old female with PsA.
a) Sagittal DECT Iodine Map of the middle finger shows inflammation in the flexor tendon sheath at middle phalanx (arrow).
b) Course of the flexor tendon is identified on corresponding PDWI of the cadaveric finger.

tenosynovitis is known to have a close relationship with RA. However, since tendon sheath runs near bones, pulleys, volar plates and other fibrous structures, the enhancement along the tendon sheath may indicate secondary tenosynovitis from classical/functional enthesitis. Hence, our results may coincide with the hypothesis that primary inflammatory sites of PsA are enthesis, which is different from RA [7].

In this study, we have noticed that there was remarkable enhancement around DIP joints. This may be explained by the fact that variable enthesis are crowded in a small DIP joint. For example, as classical enthesis, all attachment of flexor tendon, extensor tendon, radial collateral ligament, and ulnar collateral ligament are existing in the DIP joint. This finding was also consistent with the previous reports that the DIP joints are predominantly involved in PsA and are also associated with characteristic nail psoriasis [8,9]. Capsular synovitis has been regarded as the secondary inflammation due to adjacent enthesitis and the iodine accumulation of articular capsule was also often observed in DIP joint rather than the MCP and the PIP joint. Among the 22 active PsA patients, one case showed an enhancement of articular capsule of the DIP joint without any inflammation of surrounding enthesis. It can be suspected that conjoint osteoarthritis may cause iodine accumulation in the articular capsule of the DIP joint.

In our previous study, we speculated that the linear enhancement surrounding the joint space on DECT images represents inflammation of the joint capsular synovium [4,5]. However, this finding differs from typical capsular synovitis on CE-MR imaging, which showed enhancement not only in synovium but also joint space. Yamato et al. reported that enhancement of synovium and leakage of the contrast media into the joint space in patients with RA is a time-dependent phenomenon [10]. Our DECT Iodine Map of cadaveric finger, created by applying diluted iodine on the synovium, showed a linear enhancement around the joint space. Thereby, we believe the linear enhancement surrounding the joint space on DECT Iodine Map corresponds to capsular synovitis. We suspect that this discrepancy in capsular synovitis between CE-MR images and DECT images probably due to different timing of scanning after contrast injection because CE-CT is much quicker than MR scan. Another possibility is that the difference in the permeability between Gadolinium chelates and Iodine contrast media.

MR imaging and ultrasound (US) have been widely used to detect inflammatory lesions, but they have advantages and disadvantages compared with DECT. As one of the advantages, both MR imaging and US do not need radiation exposure. However, MR imaging tends to produce artifacts in the distal part of the peripheral joints, which are common sites for PsA. Also, the spatial resolution of MR imaging is sometimes inadequate. As for the disadvantages of US, it is an examiner-dependent modality and has limited objectiveness. Although DECT needs irradiation, it has the potential to overcome these problems with a much shorter scanning time. Especially, when it comes to PsA which frequently involves peripheral joints, high spatial resolution and the ability to reconstruct images with optimal section by DECT are beneficial.

Besides inflammatory arthritis, DECT has been applied in many musculoskeletal disorders. As to rheumatologic diseases, utility of DECT for gout and sacroiliitis has been reported. Detection of monosodium urate crystal deposition by DECT showed the high diagnostic performance of gout [11]. Diagnostic performance in the evaluation of sacroiliitis with axial spondyloarthritis by DECT was also excellent with its ability to delineate bone marrow edema [12]. Other representative application of DECT for musculoskeletal disease are traumatic bone marrow edema, tendon, metal artefact reduction, bone metastasis detection in oncologic patients, and bone mineral density measurement [13].

The major disadvantage of DECT is radiation exposure. We used tube current modulation and tin filters with high energy spectrum to reduce the radiation dose. Several studies have shown that radiation dose of DECT is maintained similar to conventional single-energy multi-detector CT [14–16]. In addition, the hands are distant from radiosensitive organs, such as the lens, breasts, reproductive organs, and hematopoietic bone marrow. Hence, the effect of repeated scans is limited. The accessibility of DECT is still facility-dependent, compared with MR or US. Finally, the use of iodine contrast material requires careful assessment of risks, such as renal function and history of allergy. However, contrast medium is also recommended on MRI for accurate evaluation of

inflammatory arthritis according to a recent publication [17].

There are several limitations in our study. First, anatomy of cadaveric finger can be affected by formalin-alcohol fixation which may have effect on strict correlation with in-vivo cases. The second limitation is that we did not analyze all fingers of PsA cases. However, our highest priority was to determine the anatomical location and identify the typical appearance of a variety of inflammatory lesions of PsA with correlating cadaveric specimen. Hence, we thought selecting thumb adding to middle finger which share the almost common anatomy with other fingers are sufficient to cover the all types of enthesis.

5. Conclusion

In conclusion, by using cadaveric specimen as a reference, DECT Iodine Map allowed to determine various inflamed anatomical structures of the hands in PsA. Majority of the inflammatory sites were consistent with either classical or functional enthesis and DECT Iodine Map could be a valid tool in evaluation of detailed inflammatory sites of PsA.

Ethical approval

This study was approved by the institutional review board (IRB number 30- 252(9273)).

The requirement for informed consent was waived because of its retrospective design.

Funding statement

There is no funding available.

CRediT authorship contribution statement

Sho Ogiwara: Conceptualization, Data curation, Investigation, Methodology, Writing – original draft. **Takeshi Fukuda:** Formal analysis, Writing – review & editing. **Reina Kawakami:** Investigation, Writing – review & editing. **Hiroya Ojiri:** Investigation. **Kunihiko Fukuda:** Conceptualization, Investigation, Writing – review & editing.

Declaration of Competing Interest

The authors report no declarations of interest.

Acknowledgments

Tohru Hashimoto Ph.D. prepared cadaveric hand and contributed anatomically in this work. Sho Takahashi Ph.D. statistically contributed to this work. We thank to Kengo Miyazaki and Ryuichi Ito for technically performing all DECT and MRI scan.

References

[1] D. Gladman, Psoriatic arthritis, Dermatol. Ther. 22 (1) (2009) 40–55.
[2] M. Haroon, P. Gallagher, O. FitzGerald, Diagnostic delay of more than 6 months contributes to poor radiographic and functional outcome in psoriatic arthritis, Ann. Rheum. Dis. 74 (6) (2015) 1045–1050.
[3] W. Tillett, D. Jadon, G. Shaddick, et al., Smoking and delay to diagnosis are associated with poorer functional outcome in psoriatic arthritis, Ann. Rheum. Dis. 72 (8) (2013) 1358–1361.
[4] T. Fukuda, Y. Umezawa, A. Asahina, et al., Dual energy CT Iodine Map for delineating inflammation of inflammatory arthritis, Eur. Radiol. 27 (12) (2017) 5034–5040.
[5] T. Fukuda, Y. Umezawa, S. Tojo, et al., Initial experience of using dual-energy CT with an iodine overlay Image for hand psoriatic arthritis: comparison study with contrast-enhanced MR imaging, Radiology 284 (1) (2017) 134–142.
[6] M. Benjamin, D. McGonagle, The anatomical basis for disease localisation in seronegative spondyloarthropathy at entheses and related sites, J. Anat. 199 (5) (2001) 503–526.
[7] D.B. Abrar, C. Schleich, R. Brinks, et al., Differentiating rheumatoid and psoriatic arthritis: a systematic analysis of high-resolution magnetic resonance imaging features—Preliminary findings, Skeletal Radiol. 50 (3) (2021) 531–541.
[8] D. McGonagle, R.J. Lories, A.L. Tan, et al., The concept of a "synovio-entheseal complex" and its implications for understanding joint inflammation and damage in psoriatic arthritis and beyond, Arthritis Rheum. 56 (8) (2007) 2482–2491.
[9] D. McGonagle, A.L. Tan, M. Benjamin, The nail as a musculoskeletal appendage-implications for an improved understanding of the link between psoriasis and arthritis, Dermatology 218 (2) (2009) 97–102.
[10] M. Yamamoto, K. Tamai, T. Yamaguchi, et al., MRI of the knee in rheumatoid arthritis: Gd-DTPA perfusion dynamics, J. Comput. Assist. Tomogr. 17 (5) (1993) 781–785.
[11] G. Mihaela, W.G. Johannes, M. Jaap, The fiagnostic performance of dual energy CT for diagnosing gout: a systematic literature review and meta-analysis, Rheumatology 58 (12) (2019) 2117–2121.
[12] W. Haijun, Z. Guangfeng, S. Lei, et al., Axial spondyloarthritis: dual-energy virtual noncalcium CT in the detection of bone marrow edema in the sacroiliac joints, Radiology 290 (1) (2019) 157–164.
[13] I. Simonetti, F. Verde, L. Palumbo, et al., Dual energy computed tomography evaluation of skeletal traumas, Eur. J. Radiol. 134 (January) (2021), 109456, https://doi.org/10.1016/j.ejrad.2020.109456. Epub 2020 Dec 1.
[14] T. Henzler, C. Fink, S.O. Schoenberg, et al., Dual-energy CT: radiation dose aspects, AJR Am. J. Roentgenol. 199 (5) (2012) 16–25.
[15] N.M. Kulkarni, D.F. Pinho, A.R. Kambadakone, et al., Emerging technologies in CT-radiation dose reduction and dual-energy CT, Semin. Roentgenol. 48 (3) (2013) 192–202.
[16] M.A. Jepperson, J.G. Cernigliaro, S.H. Ibrahim, et al., In vivo comparison of radiation exposure of dual-energy CT versus low-dose CT versus standard CT for imaging urinary calculi, J. Endourol. 29 (2) (2015) 141–146.
[17] W. Stomp, A. Krabben, D. van der Heijde, et al., Aiming for a simpler early arthritis MRI protocol: can Gd contrast administration be eliminated? Eur. Radiol. 25 (5) (2015) 1520–1527.